Desalination and Water Treatment
www.deswater.com
doi: 10.5004/dwt.2021.27840

242 (2021) 293–303
December

Preparation of calcium alginate-graphene oxide composite and its application for the removal of Maxilon Blue

Dewan Md. Mahmudunnabi[a], Md. Zahangir Alam[a], Tasrina R. Choudhury[b], Mohammad Nurnabi[a,*]

[a]*Department of Applied Chemistry and Chemical Engineering, University of Dhaka, Dhaka 1000, Bangladesh, emails: nnabi@du.ac.bd (M. Nurnabi), dmmnabidu@gmail.com (D. Md. Mahmudunnabi), zahangir@du.ac.bd (M.Z. Alam)*
[b]*Analytical Chemistry Laboratory, Chemistry Division, Atomic Energy Centre, Dhaka, Bangladesh, email: tasrina_rabia@yahoo.com*

Received 16 April 2021; Accepted 18 September 2021

ABSTRACT

Although graphene oxide (GO) showed excellent adsorption capacities for a few model dyes and heavy metals, its application is limited due to high dispersibility in an aqueous system. In this article preparation of non-dispersible calcium alginate-graphene oxide (CA-GO) composite, its characterization and application for adsorption of an industrial dye have been presented. The CA-GO composite was prepared by adding a mixture of GO with sodium alginate and $CaCO_3$ (SA:$CaCO_3$:GO = 10:2.5:1) to 2% HCl. The prepared composite was characterized by scanning electron microscopy, X-ray diffraction and Fourier transform infrared spectroscopy analysis. The surface charge of the composite was also determined by zeta potential analysis. The adsorption properties of the composite were investigated for an industrially used cationic dye, Maxilon Blue (GRL) (MBG). Effects of dye concentration, contact time, adsorbent dosage, pH of dye solution and temperature on adsorption capacity of the composite were studied. The equilibrium of the process preferably followed the Langmuir model. The theoretical maximum adsorption capacity was 1,253.13 mg/g at pH 7.0. For the mechanism of dye adsorption, the data fitted perfectly with a pseudo-second-order kinetic model. Thermodynamic studies revealed that the adsorption of MBG on CA-GO composite was spontaneous and physical in nature. The exhausted adsorbent was regenerated by simple treatment with 2% HCl followed by washing with demineralized water and the regenerated composite showed almost similar adsorption capacity.

Keywords: Graphene oxide; Calcium alginate; Composite; Adsorption capacity; Adsorption isotherm; Zeta potential

1. Introduction

Bangladesh is the second-largest readymade garments exporter in the world and employs about 4.2 million people, mostly women. As a result, this sector has a significant impact on the national gross domestic product (GDP) of Bangladesh. The current export value of textile products is nearly 28 billion USD per year and is expected to rise to 50 billion USD by 2021 [1,2]. As the demand for textile products has been increased due to the increased population, the discharge of textile wastewater has also increased proportionally, causing severe water pollution. During the textile dyeing process 10%–15% of the dyes remain unused and about 2% of them enter into the effluent directly [3–5]. These dyes are persistent in nature as they are non-degradable, very stable to light and other environmental conditions. Ultimately some dyes enter into the food chain, cause harm to living beings due to several health risks such as toxicity, impairment of the human immune system, skin irritation, sneezing and asthma [6, 7]. So, it is essential to remove these

* Corresponding author.

coloring materials from textile effluents before disposal. Some techniques such as biodegradation, adsorption, ion exchange and catalytic degradation are applied to remove dyes from wastewater. However, so far the most used one is the adsorption technique due to its simplicity and high effectiveness [8]. Recently we reported graphene oxide (GO) as an excellent adsorbent for Reactive Blue 21 [9] and previously many researchers documented that graphene oxide, graphene and their derivatives showed high adsorption capacities towards heavy metals and dyes from aqueous solutions [10–15]. GO has some remarkable properties such as high specific surface area, good chemical stability, etc. In the structure of GO, there are many hydrophilic polar groups [16]. So, it is highly dispersible in water and its separation and recycling are difficult. Thus immobilization of GO with a suitable polymer would be beneficial. Sodium alginate (SA) is a naturally occurring linear polysaccharide, which is water-soluble and possesses poor mechanical properties and thermal stability. These disadvantages of SA can be overcome by incorporating organic or inorganic nanoparticles into the SA matrix [17] and cross-linking with bivalent metal ions. Thus cross-linking with Ca^{2+} and simultaneous incorporation of GO afforded water-insoluble and stable calcium alginate-graphene oxide (CA-GO) composite, which was successfully used as an adsorbent for Methylene blue [18]. CA was also used to immobilize activated carbon [19], carbon nanotubes [20] and used as adsorbents for heavy metals and organic pollutants. To the best of our knowledge previously developed CA-GO adsorbents were applied to a few model dyes only, not for any industrial dye.

In the present investigation, a CA-GO composite was prepared, characterized and applied to the adsorption of an industrial dye namely Maxilon Blue (GRL) and extremely high adsorption capacity of the prepared composite at neutral pH was observed.

2. Experimental

2.1. Materials

Maxilon Blue (GRL) (MBG) dye was obtained from Interstoff Apparels Ltd., Gazipur, Bangladesh. The chemical structure of the dye is shown in Fig. 1. Here graphite powder was oxidized to prepare to GO. To oxidize graphite powder, H_2SO_4 (98%), HNO_3 (65%), $NaNO_3$, $KMnO_4$ and H_2O_2 (30%) were used. H_2SO_4 and HNO_3 were bought from Active Fine Chemicals (Bangladesh), $NaNO_3$ was obtained from Unichem (China), while $KMnO_4$ from Merck (Germany), H_2O_2 and graphite powder from Merck (India) and sodium alginate from Research Lab (India) Fine Chem Industries.

2.2. Preparation of graphene oxide and its composite

GO was prepared by modified Hummers' method mentioned elsewhere [9]. Briefly, graphite powder (10.0 g), $KMnO_4$ (30.0 g) and $NaNO_3$ (5.0 g) were added slowly over a period of 2 h to a flask placed in a water bath containing H_2SO_4–HNO_3 (3:1 ratio, 50 mL) under vigorous stirring in a magnetic stirrer and left overnight. Then deionized (DI) water (200 mL) was added and stirred for 3 h until a deep brown mixture was formed. To the mixture, DI water (200 mL) and 30% H_2O_2 (50 mL) were added with continuous stirring followed by the addition of 5% HCl (500 mL) to afford GO as a suspension. The mixture was washed with DI water to adjust the pH at 7.0.

To prepare the composite, graphene oxide (500 mg) was dispersed in DI water (250 mL) and sonicated. Then Na-alginate (5 g) and $CaCO_3$ (1.25 g) were mixed with it and the mixture was added dropwise to 2% HCl which produced effervescence and afforded CA-GO composite. The composite was washed with distilled water.

2.3. Characterization methods

The presence of functional groups in the composite was determined with Fourier transform infrared spectroscopy (FT-IR) (Prestige-21, Shimadzu, Japan). A scanning electron microscope (JSM-6010PLUS/LA) was used to study the morphology of the composite. X-ray diffraction (XRD) was also measured (Ultima IV, Cu Kα radiation, 40 kV, 1.64 mA, λ = 0.154 nm, 5°–100°). The surface charge of the composite as a function of pH was also measured by Malvern Zetasizer (Nano-ZS analyzer).

2.4. Adsorption of MBG on CA-GO composite

2.4.1. Calibration curve

At first, a stock solution of the dye MBG of 1,000 mg/L was prepared. Then standard dye solutions of 5, 10, 25, 50 and 75 mg/L were prepared by dilution. Absorbances of the standard solutions (for calibration), test solutions and solutions after adsorption were measured at 554 nm in a spectrophotometer (UV-1700 Pharma Spectrophotometer, Shimadzu, Japan). The calibration curve was obtained by plotting concentration vs. absorbance.

2.4.2. Effect of pH

To determine the effect of pH on the adsorption capacity of the composite, experiments were carried out at 5 different pH. For this, 10 mL of 700 mg/L dye solutions were taken in five different conical flasks and pH was adjusted from 2–10 using dilute HCl or NaOH. Then 9 mg of CA-GO composite was added to the solutions. Then mixtures were shaken for 60 min at 200 rpm. After shaking the mixtures were filtered and the concentration of the filtrates was calculated using the calibration curve. The adsorption capacities at different pH were calculated using Eqs. (1) and (2).

$$q = \frac{\left(C_0 - C_t\right)V}{W} \tag{1}$$

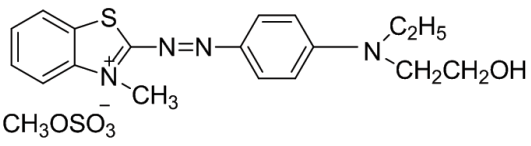

Fig. 1. Molecular structure of Maxilon Blue.

$$q_e = \frac{(C_0 - C_e)V}{W} \quad (2)$$

where C_0, C_e, C_t represent the dye concentrations at the initial stage, equilibrium stage and at time t, respectively. V and W are the volume of dye solution (L) and mass (g) of the adsorbent, respectively.

2.4.3. Effect of adsorbent dosage

To determine the optimum dosage of CA-GO composite for the adsorption of MBG, 4 experiments were carried out. In each flask, 10 mL of 1,000 mg/L dye solution was taken and pH was adjusted at 7. Then 5–20 mg of the composite were added to the solutions and shaken for 60 min at 200 rpm. After shaking, the mixtures were filtered and the concentrations of the filtrates were calculated using the calibration curve. Then the adsorption capacities and % of removals were calculated using Eqs. (1) and (3), respectively.

$$\%\ \text{removal} = \frac{(C_0 - C_t)}{C_0} \times 100 \quad (3)$$

2.4.4. Effect of dye concentration and contact time

To study the effect of contact time and dye concentration on the adsorption of MBG on CA-GO composite, a set of 7 experiments were carried out. For this, 10 mL of 500 mg/L dye solution was taken in each conical flask and pH was adjusted at 7. Then 9 mg of the composite were added to each solution and left under shaking at 200 rpm in various intervals of time ranging from 10–90 min. After shaking the mixtures were filtered and the concentrations of the filtrates were calculated using the calibration curve. The adsorption capacities at different times were calculated using Eq. (1). Effect of dye concentrations on adsorption was carried out in a similar fashion using 600, 800 and 900 mg/L of the dye solutions in the same intervals of time.

2.5. Adsorption isotherms

Both Langmuir and Freundlich isotherms were used to analyze the dye molecule distribution on the adsorbent surface [21,22]. The linear form of the Langmuir isotherm is:

$$\frac{C_e}{q_e} = \frac{1}{q_m b} + \frac{1}{q_m} C_e \quad (4)$$

where C_e is equilibrium concentration and b is Langmuir constant. q_e and q_m are equilibrium adsorption capacity and theoretical maximum adsorption capacity, respectively.

Theoretical maximum adsorption capacity q_m was calculated by plotting C_e/q_e vs. C_e according to the Langmuir model.

The value of separation factor R_L was calculated to determine the favorable nature of the adsorption process. R_L value was calculated using Eq. (5).

$$R_L = \frac{1}{1 + C_m b} \quad (5)$$

where C_m is the maximum initial dye concentration in the experiments.

Freundlich isotherm assumes multilayer and non-uniform distribution of the adsorbate molecules. The linear form of Freundlich isotherm is:

$$\ln q_e = \ln K_F + \frac{1}{n} \ln C_e \quad (6)$$

where n is Freundlich constant and K_F is maximum theoretical adsorption capacity (mg/g).

2.6. Adsorption kinetics

In this study pseudo-first-order and pseudo-second-order kinetic models were also studied [23,24]. The pseudo-first-order model was studied by plotting $\log(q_e - q_t)$ vs. t according to Eq. (7).

$$\log(q_e - q_t) = \log q_e - \frac{K_1}{2.303} t \quad (7)$$

where q_e and q_t are equilibrium adsorption capacity and adsorption capacity at time t. K_1 is the rate constant (1/min) for pseudo-first-order adsorption.

The pseudo-second-order model was tested by plotting t/q_t vs. t according to Eq. (8).

$$\frac{t}{q_t} = \frac{1}{K_2 q_e^2} + \frac{1}{q_e} t \quad (8)$$

where K_2 is the rate constant (g/mg min) for pseudo-second-order adsorption.

2.7. Thermodynamic analysis of the adsorption process

The thermodynamics of the adsorption process was studied by carrying out the adsorption of MBG on CA-GO at three different temperatures (303, 313 and 323 K). For each temperature, 10 mL of 900 mg/L MBG solution were taken in 7 different conical flasks and pH was adjusted at 7. Then 9 mg of CA-GO composite was added to each flask and left under shaking for different time periods ranging from 10–90 min. The solutions were filtered and the absorbance of each solution was measured and the remaining dye concentrations were obtained using the calibration curve.

The Gibbs free energy change ($\Delta G°$) was calculated according to Eqs. (9) and (10).

$$\Delta G° = -RT \ln k_d \quad (9)$$

where R = universal gas constant (8.314 J mol^{-1} K^{-1}), k_d = the distribution constant for the equilibrium sorption and T = the absolute temperature (K).

$$k_d = \frac{q_e}{c_e} \quad (10)$$

The van't Hoff equation [Eq. (11)] was used to calculate the average standard enthalpy change ($\Delta H°$) and entropy change ($\Delta S°$). The linear form of van't Hoff equation is:

$$\ln k_d = -\frac{\Delta H^\circ}{RT} + \frac{\Delta S^\circ}{R} \quad (11)$$

By plotting $\ln k_d$ vs. $1/T$, a straight line was obtained. The value of ΔH° and ΔS° were obtained from the slope and intercept, respectively.

2.8. Regeneration of the adsorbent

50 mg of the exhausted CA-GO was soaked in 2% HCl (20 mL) and left for 30 min under shaking. The material was separated by filtration and washed with DI water until neutralization. The regenerated adsorbent was then dried in an oven at 50°C for 2 h, cooled in desiccators and stored for further adsorption study.

3. Result and discussion

3.1. Preparation of calcium alginate-graphene oxide composite

Graphene oxide was synthesized by oxidizing graphite powder with a mixture of concentrated H_2SO_4 and HNO_3. To complete the oxidation $KMnO_4$, $NaNO_3$ and H_2O_2 were also added. During the oxidation process, the oxygenated functional group (–COOH group) was introduced into the GO structure [25] and simultaneously layer separation of graphite powder took place and exfoliated GO was obtained.

CA-GO composite was prepared by adding a mixture of Na-alginate, GO and $CaCO_3$ drop-wise into 2% HCl. SA is hydrophilic and water-soluble and has gel-forming properties, however, during the composite formation sodium ions are replaced by bivalent calcium ions and a good cross-linking occurred between linear polysaccharide chains of alginate [17,26] and due to this cross-linking a three-dimensional scaffold resulted. GO was attached to the scaffold through H-bonding and thus CA-GO composite was formed (Fig. 2). During the process, the reaction of calcium carbonate and HCl liberated CO_2 gas, which was escaped as bubbles and made the composite porous.

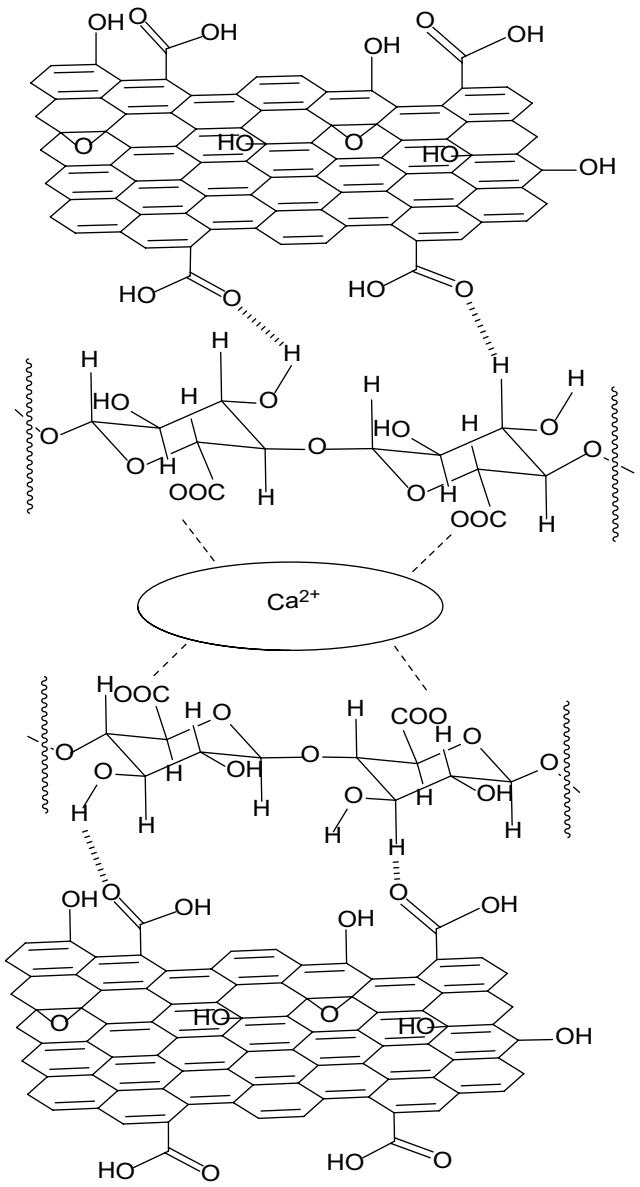

Fig. 2. Structure of CA-GO composite showing the interaction between GO-alginate cross-linking with Ca^{2+}.

3.2. Characterization of CA-GO composite

3.2.1. FT-IR spectroscopic analysis

From the FT-IR spectrum of CA-GO composite (Fig. 3) vibrational peaks were observed at 3,403; 1,615 and 1,076 cm^{-1} corresponding to the presence of –OH, aromatic C=C and C–O–C groups, respectively. In GO spectrum, the peak observed at 3,431; 2,919; 1,720; 1,615; 1,405 and 1,068 cm^{-1} which are attributable to stretching vibrations in O–H, C–H, C=O, aromatic C=C and C–O–O functionalities respectively [26–28]. In the case of SA characteristic peaks at 3,417; 1,636 and 1,075 cm^{-1}, are assignable to –OH, carboxylate group (symmetric and asymmetric vibrations) and C–O–C vibrations. It is worth noting that for the CA-GO composite a significant shift of O–H took place, which confirms the occurrence of H-bonding in the composite [26].

3.2.2. Scanning electron microscopic observations

The morphology of the CA-GO composite was studied with scanning electron microscopy (SEM). Previous SEM studies of SA films revealed smooth and homogeneous morphology, while the composite had rough morphology [25]. In the case of our composite, wrinkled GO sheets were observed in the CA-GO composite (Fig. 4), which supports the embedded GO sheets into the composite.

3.2.3. XRD analysis of SA and CA-GO composite

The XRD peaks of sodium alginate (SA), GO and CA-GO is presented in Fig. 5. SA showed two broad peaks at 2θ = 13.38° and 20.98° corresponding to the interlayer spacing of 6.61 and 4.23 Å and indicates a rather amorphous structure of SA. For the CA-GO composite, peaks were nearly identical to that of SA, suggesting that incorporation of GO did not change the amorphous structure of SA [26].

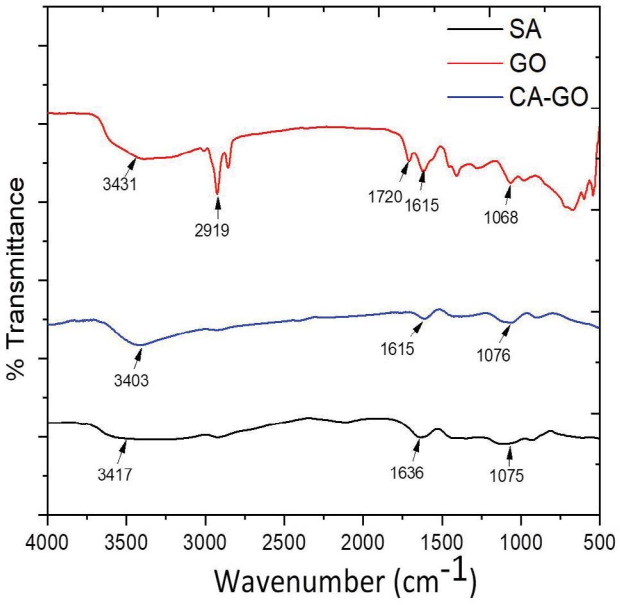

Fig. 3. FT-IR spectrum of SA, GO and CA-GO.

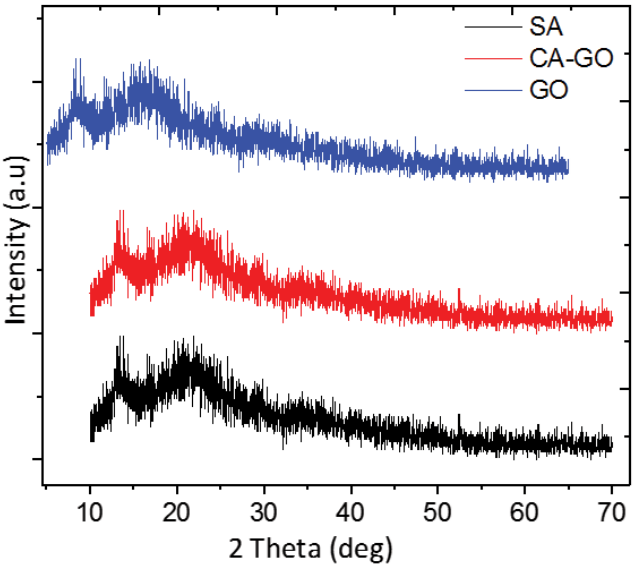

Fig. 5. XRD patterns of SA, GO and CA-GO composite.

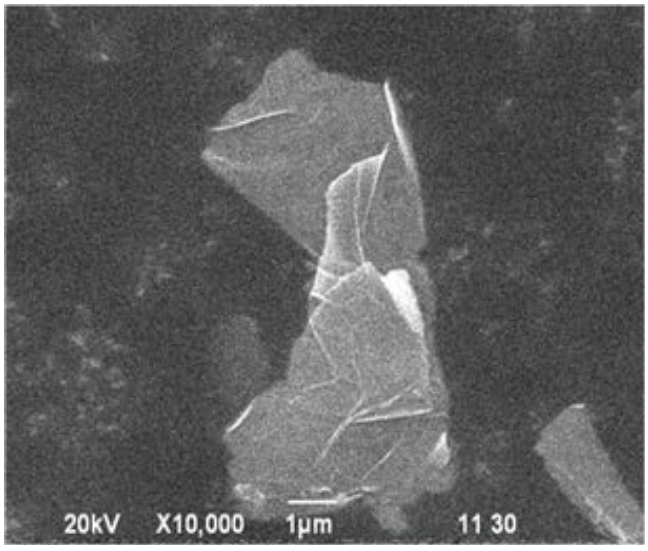

Fig. 4. SEM image of CA-GO composite.

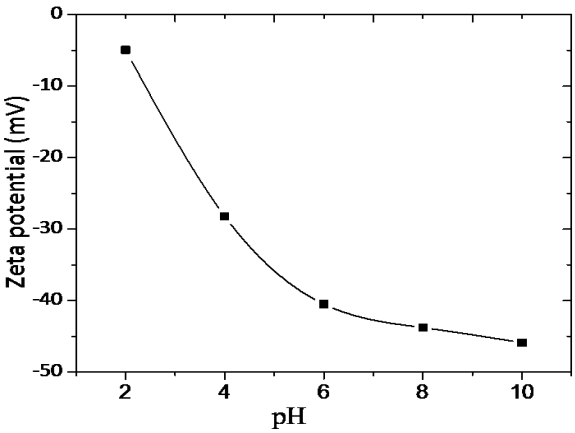

Fig. 6. Zeta potential value of CA-GO at different pH.

3.2.4. Zeta potential value of CA-GO composite

Zeta potential represents surface charge, which is a significant characterization of functional materials to demonstrate the adsorption capacities of different analytes. In the present investigation, the zeta potential of CA-GO composite as a function of pH (2–10) was also studied. For this study, CA-GO composite was dispersed in DI water and pH was at the range of 2–10 by using dilute HCl or NaOH. The results showed that (Fig. 6) the zeta potential values of the composite were negative (–4.93 to –45.9 mV) over the whole pH range with an increase of pH from 2 to 10. It is thus evident that the negative surface charge suddenly increases from pH 2 to 6 and then it remains at a value of around –40 mV on a further increase of pH. This trend of zeta potential value suggests the ionization of the –COOH group of the GO moiety in the composite.

3.3. Adsorption of dye MBG on CA-GO composite

3.3.1. Effect of pH

The effect of pH on adsorption of MBG by CA-GO composite was studied at the pH range of 2–10 and adding 9 mg of composite for 10 mL 700 mg/L dye solution. The minimum adsorption capacity of the CA-GO composite was found to be 338.57 mg/g at a pH of 2. The adsorption capacity sharply increased until pH of 6 and was almost constant up to a pH of 10. The maximum adsorption capacity was 795.10 mg/g at a pH of 10 (Fig. 7).

At low pH, some of the carboxyl groups of GO moiety of the composite get protonated (Fig. 8), as a result the positive charge developed on the –COOH group [29]

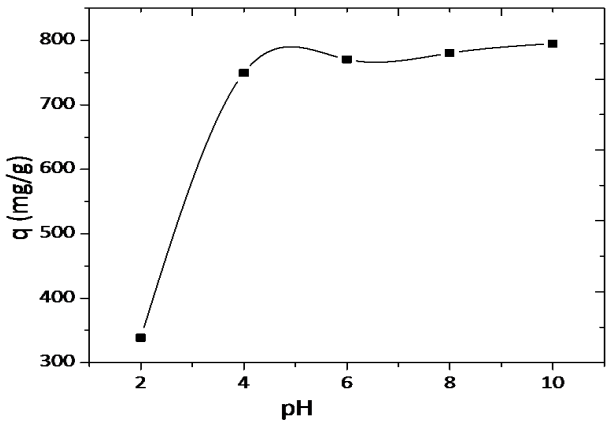

Fig. 7. Effects of pH on adsorption capacity of composite (700 mg/L dye concentration; 9 mg CA-GO/10 mL dye solution at 303 K temperature).

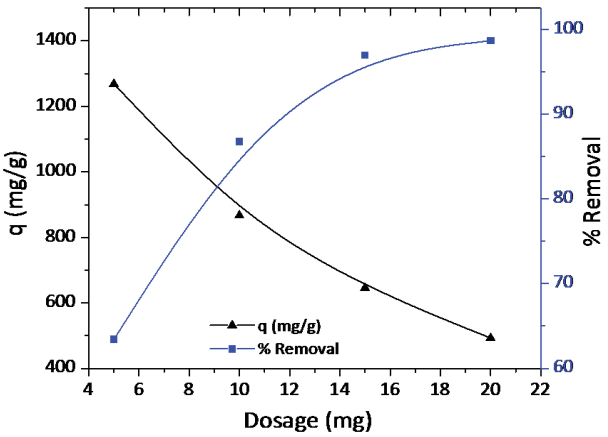

Fig. 9. Effects of dosage of CA-GO composite (mg/10 mL 1,000 mg/L dye solution), pH was 7 and temperature was 303 K.

although the overall surface charge is slightly negative. Thus the cationic dye MBG was less attracted at the low pH and led to lower adsorption. With the increasing pH, carboxyl groups got dissociated extensively and the surface became highly negatively charged [30], which caused strong electrostatic attraction of the cationic dye and led to high adsorption capacity.

Here, the adsorption capacity remained steady at a pH range of 6–10 as it was assumed that at pH of 6 most of the carboxyl groups of GO got deprotonated to form carboxylate ion ($–COO^-$) and showed the maximum adsorption and further increase of pH did not increase the extent of deprotonation [31] significantly and thus adsorption remained almost constant.

3.3.2. Effect of adsorbent dosage

The effect of CA-GO dosage on adsorption of MBG was studied at pH 7 and adding 5–20 mg of CA-GO composite into 10 mL of 1,000 mg/L dye solution. It was apparent that the adsorption capacity decreased with the increase of adsorbent dosage. But percentage removal of dye increased with the increase of adsorbent dosage (Fig. 9). This observation is due to the fact that with the increasing dosage, the amount of adsorbate per unit mass of adsorbent decreased and demonstrated adsorption capacity [32]. The point of intersection of the values of adsorption capacities and % removals was considered as optimum dosage. The dosage 9 mg/10 mL solution demonstrated the best adsorption capacity and the best percentage removal. So, the dosages of 9 mg/10 mL dye solution were maintained throughout the study.

3.3.3. Effect of dye concentration and contact time

The effects of dye concentration and contact time on adsorption of MBG by CA-GO composite were studied taking 10 mL of dye solutions in 7 different 25 mL conical flasks and 9 mg of CA-GO were added in each flask and left for 10–90 min at pH 7. Four concentrations such as 500, 600, 800 and 900 mg/L were employed to observe the effect of concentration and time. It was observed that within 30 min the adsorption reached almost the highest value. In the beginning, more active sites of adsorbent were available and with increasing time these sites became saturated, so CA-GO showed high adsorption capacities initially until it reached equilibrium and became constant (Fig. 10). High initial dye concentration also resulted in high adsorption capacity due to the high concentration gradient of the dye between the adsorbent surface and in the bulk solution [33], leading to high mass transfer.

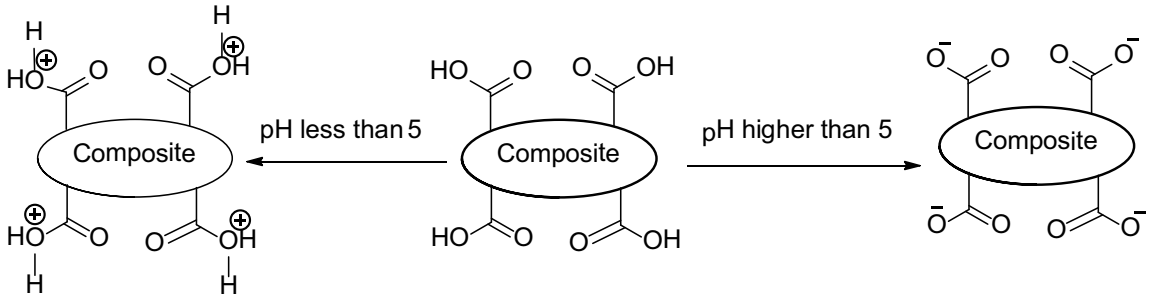

Fig. 8. Effect of pH on the surface charge of CA-GO composite.

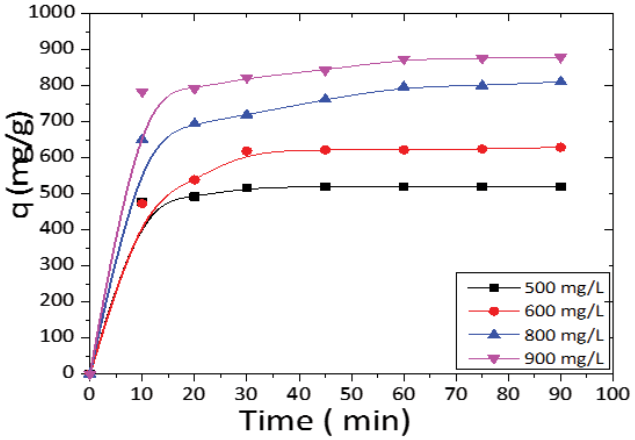

Fig. 10. Effect of dye concentration and time on adsorption capacity of CA-GO (9 mg/10 mL dye solution) pH was 7 at 303 K.

3.4. Adsorption isotherms

To get an assumption, about the distribution of dye MBG molecules on the CA-GO surface both Langmuir and Freundlich isotherm models were used. Langmuir model was tested by plotting C_e/q_e vs. C_e according to Eq. (4) and a linear relation between C_e/q_e and C_e was observed (Fig. 11a) with an excellent regression factor (R^2 = 0.9982).

The theoretical maximum adsorption capacity, q_m calculated from Langmuir isotherm was found to be 1,253.13 mg/g. The separation factor R_L is calculated using Eq. (5) and the value was 0.040, which indicates a very favorable monolayer adsorption process [13].

The experimental data were also tested for the multilayer adsorption mechanism employing the Freundlich isotherm by plotting $\ln C_e$ vs. $\ln q_e$ according to Eq. (6) and a linear relationship was observed (Fig. 11b) with a good regression coefficient (R^2 = 0.984). The value of n was also calculated using Eq. (6) and was found to be 2.58 which showed that the adsorption was moderate to good [13].

Table 1
Theoretical values of q_m, b, R_L, n, K_F and R^2 of CA-GO composite for dye MBG

Model	Parameters	Results
Langmuir isotherm	q (mg/g)	1,253.13
	R^2	0.9982
	b (L/mg)	0.027
	R_L	0.040
Freundlich isotherm	R^2	0.9840
	n	2.58
	K_F (mg/g)	141.43

The values of Langmuir isotherm and Freundlich isotherm parameters are represented in Table 1 and it was evident that the adsorption of dye MBG on CA-GO preferably followed the Langmuir model. The adsorption capacity of the composite CA-GO synthesized in this study is compared with previous works and provided in Table 2.

To ascertain the benefit of using the CA-GO composite, a comparison of adsorption capacities was made with pure sodium alginate (Fig. 12). The comparison was made by using the same dosage of 9 mg/10 mL of CA-GO and sodium alginate into the dye solutions of concentration 800 mg/L and at pH 7. Both the experiments were left for the same contact time of 60 min. From Fig. 12, it is evident that the CA-GO composite showed much-more higher adsorption capacity than that of sodium alginate.

3.5. Adsorption kinetics for adsorption of dye MBG on CA-GO composite

In this study, first-order and second-order models were employed to understand the underlying mechanism of

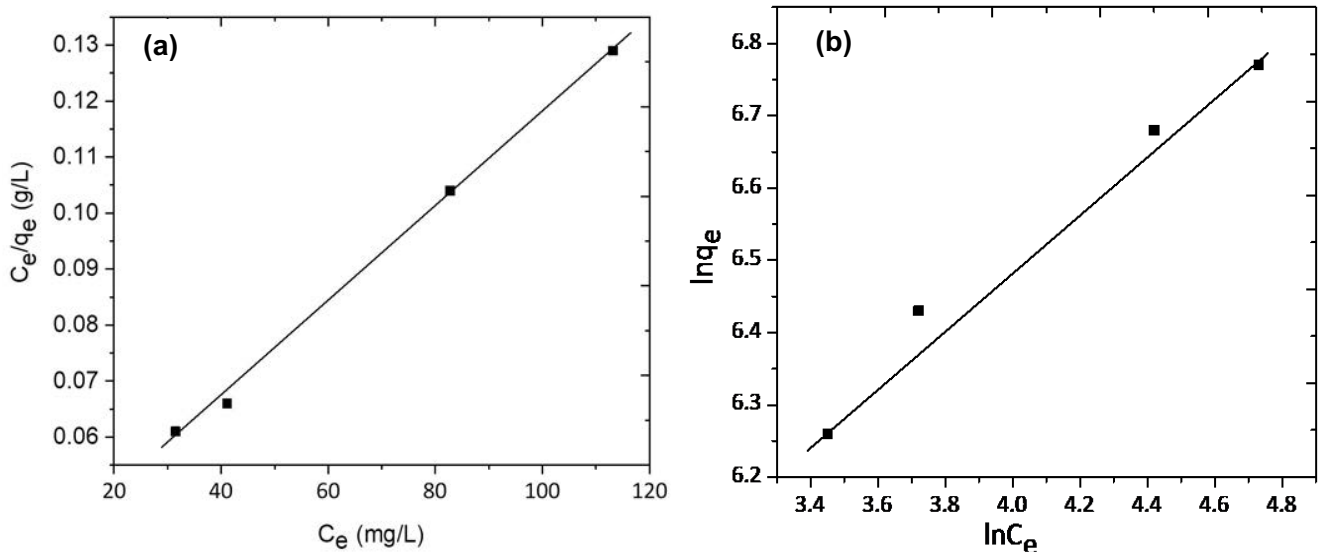

Fig. 11. Langmuir isotherm (a) and Freundlich isotherm (b) at 303 K.

Table 2
Adsorption capacities of different adsorbents with optimum pH and time

Name of adsorbent	Optimum pH and time (min)	Adsorption capacity (mg/g)	Reference
Commercial activated carbon	pH = 7.4, 35 min	980.3 mg/g for Methylene blue	[34]
Graphene oxide	pH = 9, 90 min	1.939 mg/mg for Methylene blue	[35]
Magnetic graphene oxide	pH = 10, 500 min	64.23 mg/g for Methylene blue	[14]
Superparamagnetic graphene oxide	pH = 3–10, 30 min	167.2 mg/g for Methylene blue	[10]
Thermally reduced graphene	pH = 6.2, 60 min	89.3 mg/g for Methyl orange	[13]
Multi-walled carbon nanotubes	pH = 10, 120 min	260.7 mg/g for Maxilon Blue (GRL)	[36]
CA-GO composite	pH = 7, 30 min	1,253.13 mg/g for Maxilon Blue	This study

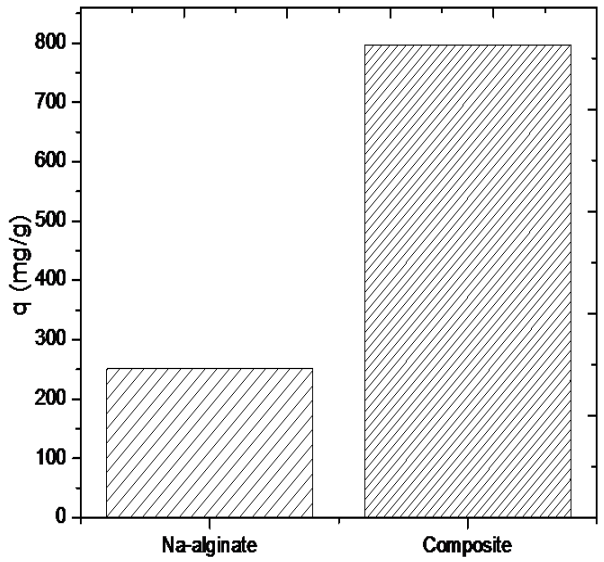

Fig. 12. Comparison of adsorption capacity of SA and CA-GO composite.

dye adsorption on the composite. The pseudo-first-order model is obtained by plotting $\log(q_e - q_t)$ vs. t according to Eq. (7) (Fig. 13 a). Whereas t/q_t vs. t was plotted to obtain a pseudo-second-order model (Fig. 13b).

From the plots, the kinetic parameters were calculated and presented in Table 3. It was clear that for the first-order model the R^2 value is low. Moreover, the calculated adsorption capacities are much lower than the experimental values. While for the second-order model the R^2 value is very high and the calculated adsorption capacities match well with the experimental values. Thus it is conclusive that the adsorption process is controlled by pseudo-second-order kinetics indicating that the overall process proceeds through sharing of electrons between adsorbent and adsorbate [37].

3.6. Thermodynamic analysis for adsorption of dye MBG on CA-GO composite

Thermodynamic analysis such as the feasibility and spontaneity of the adsorption process was carried out by calculating standard free energy change, enthalpy change and entropy change. Data were accumulated by conducting

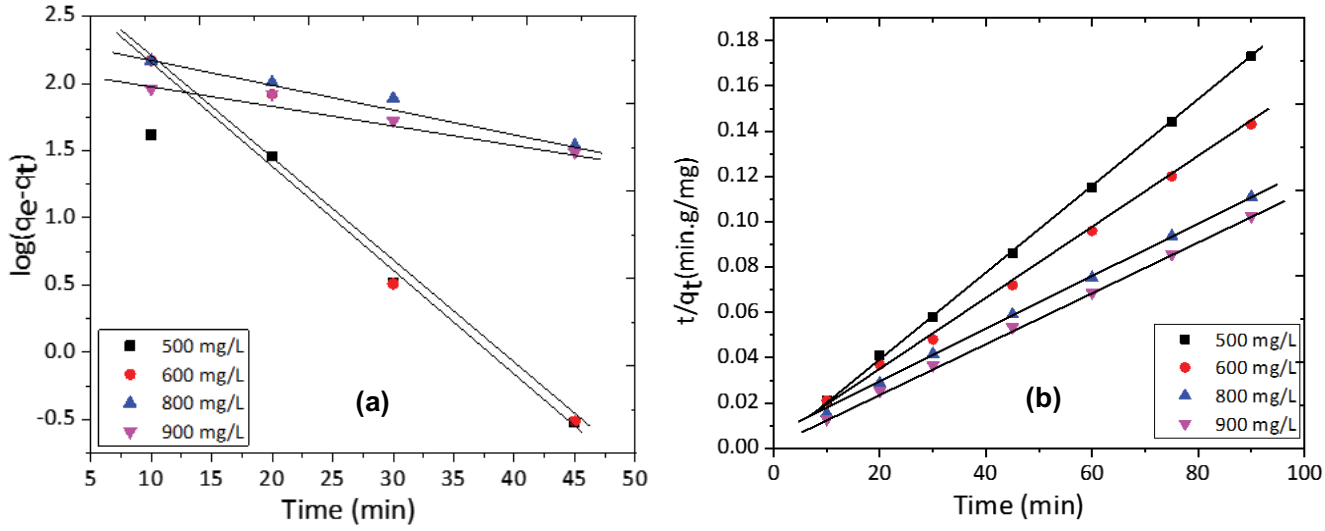

Fig. 13. First-order (a) and second-order kinetics (b) at 303 K.

Table 3
Kinetic parameters for the adsorption of MBG on CA-GO

Models	Parameters	C_0, mg/L			
		500	600	800	900
Pseudo-first-order	$q_{e,exp}$ (mg/g)	520.56	622.10	796.94	874.26
	$q_{e,cal}$ (mg/g)	293.56	266.26	233.40	139.28
	K_1 (1/min)	0.149	0.189	0.040	0.033
	R^2	0.9162	0.9226	0.9002	0.906
Pseudo-second-order	$q_{e,exp}$ (mg/g)	520.56	622.10	796.94	874.26
	$q_{e,cal}$ (mg/g)	526.32	666.67	833.33	909.09
	K_2 (g/mg min)	0.0019	0.00049	0.00029	0.00045
	R^2	0.9998	0.9989	0.9993	0.9996

adsorption experiments at three different temperatures (303, 313 and 323 K). Gibb's free energy change ($\Delta G°$) was calculated according to the Eq. (10) and van't Hoff equation [Eq. (11)] was used to obtain the standard enthalpy change ($\Delta H°$) and entropy change ($\Delta S°$) of the adsorption process. The value of $\Delta H°$ was found to be –47.39 kJ/mol and $\Delta S°$ was found to be –0.139 kJ/mol K. The values of $\Delta G°$ at different temperatures are listed in Table 4.

The values of $\Delta G°$ were negative over the range of temperature and it was evident that the adsorption of MBG on CA-GO is spontaneous. $\Delta G°$ values of 0 to –20 kJ/mol indicates that the adsorption process is physisorption, while the values –80 to –400 kJ/mol indicate the chemisorption process [13, 38]. The $\Delta G°$ values of the current investigation supported that the adsorption of MBG on CA-GO is a physisorption process.

The value of $\Delta H°$ of the process was negative and the process is considered as an exothermic one which was supported by the fact that the adsorption capacity decreased with an increase in temperature (Fig. 14).

Table 4
Thermodynamic parameters for the adsorption of MBG on CA-GO

Thermodynamic constant	Temperature (K)		
	303	313	323
$\Delta G°$ (kJ/mol)	–5.27	–3.75	–2.55

3.7. Plausible mechanism for adsorption of dye MBG on CA-GO

Well-established mechanisms for the adsorption of organic dyes on graphene-based materials are hydrogen bonding, electrostatic and π–π interactions [39]. At pH above

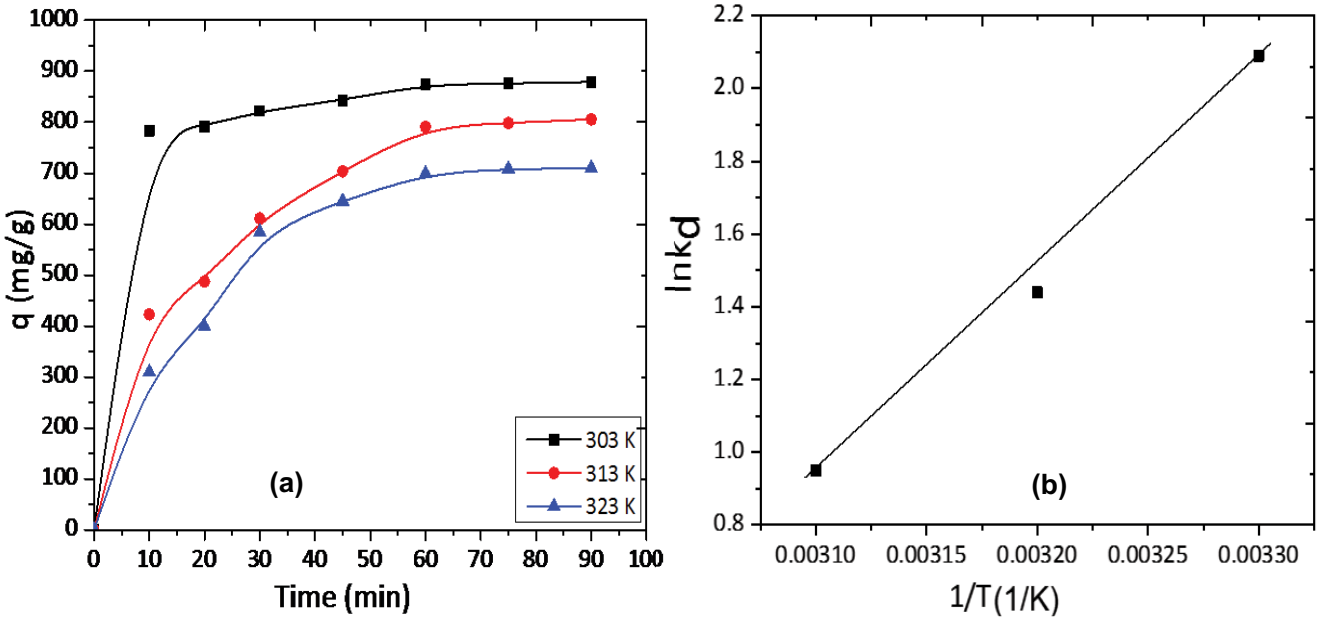

Fig. 14. The adsorption capacity of MBG on composite at different temperature (a) and van't Hoff equation (b).

5 carboxyl groups of GO moiety of the composite got dissociated and formed a negatively charged surface (Fig. 8). As a result, the composite showed strong electrostatic interaction with MBG (Fig. 15), which is a cationic dye and demonstrated very high adsorption capacities.

3.8. Regeneration and reuse of the CA-GO adsorbent

To develop an effective adsorbent it is necessary to confirm that the adsorbent can be regenerated and recycled without severe loss of its adsorption capacity. In this study, the exhausted CA-GO adsorbent was treated with 2% HCl followed by washing with deionized water until pH reached 7. Then the regenerated CA-GO composite was dried and used for further adsorption. It was assumed that in acidic solution the adsorbed cationic dye was replaced by H^+ ion and resulted in desorption of the dye molecules [38]. A comparison of fresh CA-GO and regenerated one is shown in Fig. 16. Fresh CA-GO showed the adsorption capacity of 874.26 mg/g while the regenerated CA-GO showed the adsorption capacities of 683.27, 667.84, 664.31, 653.43 and 657.38 mg/g of 1st, 2nd, 3rd, 4th and 5th recycle (Fig. 16) respectively.

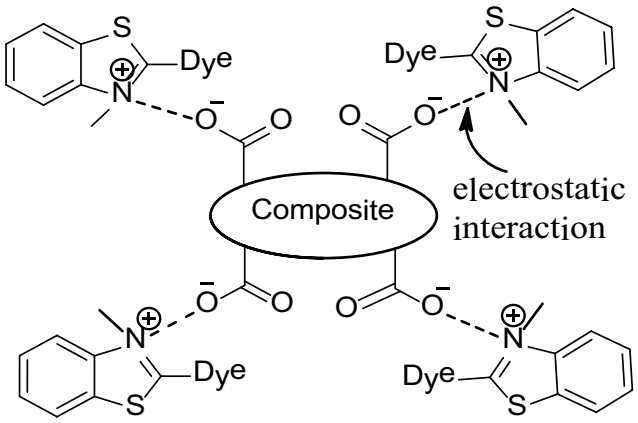

Fig. 15. Mechanism of MBG adsorption on CA-GO.

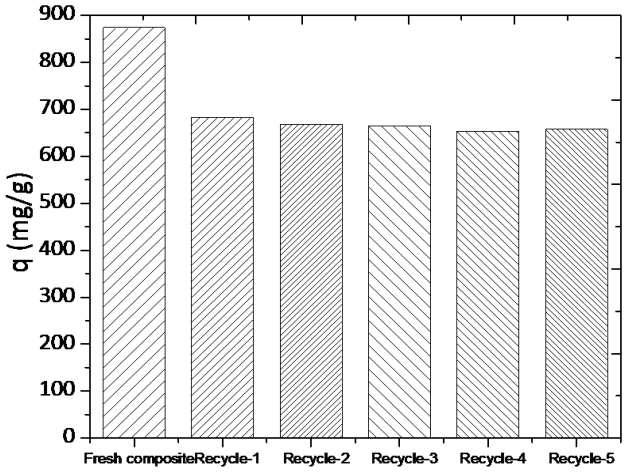

Fig. 16. Comparison of adsorption capacities of fresh and recycled CA-GO composite for dye MBG.

4. Conclusion

In the present investigation, CA-GO was synthesized and characterized with the help of infrared spectroscopy, XRD, SEM and zeta potential analysis. The composite was then employed as the adsorbent for a cationic textile dye and found extremely high adsorption capacity. The adsorption data fitted with both Langmuir and Freundlich isotherm models, however, it fitted best with the Langmuir model and the adsorption capacity was 1,253.13 mg/g at a pH of 7. Kinetic studies showed that the process is controlled by a pseudo-second-order kinetic model. Thermodynamic studies revealed that the adsorption process was spontaneous and physical in nature. The exhausted CA-GO was regenerated by treating with 2% HCl and recycled without significant loss of adsorption capacities up to fifth recycle.

Acknowledgment

The authors would like to thank the University Grants Commission of Bangladesh (UGC) for providing financial support and the Department of Applied Chemistry and Chemical Engineering, the University of Dhaka for all logistic and laboratory supports.

References

[1] M.M. Islam, A.M. Khan,Textile industries in Bangladesh and challenges of growth, Res. J. Eng. Sci., 2 (2013) 31–37.
[2] L. Hossain, S.K. Sarker, M.S. Khan, Evaluation of present and future wastewater impacts of textile dyeing industries in Bangladesh, Environ. Dev., 26 (2018) 23–33.
[3] K.Y. Foo, B.H. Hameed, An overview of dye removal via activated carbon adsorption process, Desal. Water Treat., 19 (2011) 255–274.
[4] C.I. Pearce, J.R. Lioyd, J.T. Guthire, The removal of colour from textile wastewater using whole bacterial cells: a review, Dyes Pigm., 58 (2003) 179–196.
[5] T. Robinson, G. McMullan, R. Marchant, P. Nigam, Remediation of dyes in textile effluent : a critical review on current treatment technologies with a proposal alternative, Bioresour. Technol., 77 (2001) 247–255.
[6] C. O'Neill, F.R. Hawkes, D.L. Hawkes, N.D. Lourenco, H.M. Pinheiro, W. Delee, Colour in textile effluents–sources, measurement, discharge consents and simulation: a review, J. Chem. Technol. Biotechnol., 74 (1999) 1009–1018.
[7] M.A. Hassaan, A.E. Nemr, Health and environmental impacts of dyes: mini review, 1 (2017) 64–67.
[8] W. Zhang, C. Zhou, W. Zhou, A. Lei, Q. Zhang, Q. Wan, B. Zou, Fast and considerable adsorption of Methylene blue dye onto graphene oxide, Bull. Environ. Contam. Toxicol., 87 (2011) 86–90.
[9] D.M. Mahmudunnabi, M.Z. Alam, M. Nurnabi, Removal of TURQUOISE GN from aqueous solution using graphene oxide, Desal. Water Treat., 174 (2020) 389–399.
[10] G. Xie, P. Xi, H. Liu, F. Chen, L. Huang, Y. Shi, J. Wang, A facile chemical method to produce superparamagnetic graphene oxide–Fe_3O_4 hybrid composite and its application in the removal of dyes from aqueous solution, J. Mater. Chem., 22 (2012) 1033–1039.
[11] G.K. Ramesha, A.V. Kumara, H.B. Muralidhara, S. Sampath, Graphene and graphene oxide as effective adsorbents toward anionic and cationic dyes, J. Colloid Interface Sci., 361 (2011) 270–277.
[12] A. Naseri, R. Barati, F. Rasoulzade, M. Bahram, Studies on adsorption of some organic dyes from aqueous solution onto graphene nanosheets, Iran. J. Chem. Chem. Eng., 34 (2015) 33–42.

[13] M. Iqbal, A. Abdala, Thermally reduced graphene: synthesis, characterization and dye removal applications, RSC Adv., 3 (2013) 24455–24464.
[14] J.H. Deng, X.R. Zhang, G.M. Zeng, J.L. Gong, Q.Y. Niu, J. Liang, Simultaneous removal of Cd(II) and ionic dyes from aqueous solution using magnetic graphene oxide nanocomposite as an adsorbent, Chem. Eng. J., 226 (2013) 189–200.
[15] R. Tovar-Gomez, D.A. Rivera-Ramirez, V. Hernandez-Montoya, A. Bonilla-Petriciolet, C.J. Duran-Valle, M.A. Montes-Moran, Synergic adsorption in the simultaneous removal of Acid blue 25 and heavy metals from water using a $Ca(PO_3)_2$-modified carbon, J. Hazard. Mater., 199–200 (2012) 290–300.
[16] O. Duman, C.O. Diker, S. Tung, Development of highly hydrophobic and superoleophilic fluro organothiol-coated carbonized melamine sponge/rGO composite absorbent material for the efficient and selective absorption of oily substances from aqueous environments, J. Environ. Chem. Eng., 9 (2021) 1–15.
[17] L. Nie, C. Liu, J. Wang, Y. Shuai, X. Cui, L. Liu, Effects of surface functionalized graphene oxide on the behavior of sodium alginate, Carbohydr. Polym., 117 (2015) 616–623.
[18] Y. Li, Q. Du, T. Liu, J. Sun, Y. Wang, S. Wu, Z. Wang, Y. Xia, L. Xia, Methylene blue adsorption on graphene oxide/calcium alginate composites, Carbohydr. Polym., 95 (2013) 501–507.
[19] T.Y. Kim, H.J. Jin, S.S. Park, S.J. Kim, S.Y. Cho, Adsorption equilibrium of copper ion and phenol by powdered activated carbon, alginate bead and alginate-activated carbon bead, J. Ind. Eng. Chem., 14 (2008) 714–719.
[20] Y.H. Li, F.Q. Liu, B. Xia, Q.J. Du, P. Zhang, D.C. Wang, Z.H. Wang, Y.Z. Xia, Removal of copper from aqueous solution by carbon nanotube/calcium alginate composites, J. Hazard. Mater., 177 (2010) 876–880.
[21] G. Uslu, M. Tanyol, Equilibrium and Thermodynamic parameters of single and binary mixture biosorption of lead(II) and copper(II) ions onto *Pseudomonas putida*: effect of temperature, J. Hazard. Mater., B, 135 (2006) 87–93.
[22] H.M.F. Freundlich, Over the adsorption in solution, J. Phys. Chem., 57 (1906) 385–471.
[23] J.P. Simonin, On the comparison of pseudo-first-order and pseudo-second-order rate laws in the modeling of adsorption kinetics, Chem. Eng. J., 300 (2016) 254–263.
[24] O. Duman, S. Tunc, T.G. Polat, Determination of adsorptive properties of expanded vermiculite for the removal of C.I. Basic Red 9 from aqueous solution: kinetic, isotherm and thermodynamic studies, Appl. Clay Sci., 109–110 (2015) 22–32.
[25] M. Ionita, M.A. Pandele, H. Iovu, Sodium alginate/graphene oxide composite films with enhanced thermal and mechanical properties, Carbohydr. Polym., 94 (2013) 339–344.
[26] Y. Wan, X. Chen, G. Xiong, R. Guo, H. Luo, Synthesis and characterization of three-dimensional porous graphene oxide/sodium alginate scaffolds with enhanced mechanical properties, Mater. Expres, 4 (2014) 429–434.
[27] W. Chen, L. Yan, P.R. Bangal, Preparation of graphene by the rapid and mild thermal reduction of graphene oxide induced by microwaves, Carbon, 48 (2010) 1146–1152.
[28] R. Rezaee, S. Nasseri, A.H. Mahi, R. Nabizadeh, S.A. Mousavi, A. Rashidi, A. Jafari, S. Nazmara, Fabrication and characterization of a polysulfone-graphene oxide nanocomposite membrane for arsenate rejection from water, J. Environ. Health Sci. Eng., 13 (2015) 1–11.
[29] P. Nuengmatcha, S. Chanthai, adsorption capacity of the as-synthetic graphene oxide for the removal of Alizarin Red S dye from aqueous solution, Orient. J. Chem., 32 (2016) 1399–1410.
[30] P. Bartezak, M. Norman, L. Klapiszewski, N. Karwanska, M. Kawalec, M. Baczynska, M. Wysokowski, J. Zdarta, F. Ciesielczyk, T. Jesionowski, Removal of nickel(II) and lead(II) ions from aqueous solution using peat as a low-cost adsorbent: a kinetic and equilibrium study, Arabian J. Chem., 11 (2018) 1209–1222.
[31] X. Yang, T. Zhou, B. Ren, A. Hursthouse, Y. Zhang, Removal of Mn(II) by sodium alginate/graphene oxide composite double-network hydrogel beads from aqueous solutions, Sci. Rep., 8 (2018) 1–16.
[32] A. Shukla, Y.H. Zhang, P. Dubey, J.L. Margrave, S.S. Shukla, The role of sawdust in the removal of unwanted materials from water, J. Hazard. Mater., 95 (2002) 137–152.
[33] A. Tajiki, M. Abdouss, Synthesis and characterization of graphene oxide nano-sheets for effective removal of phthalocyanine from aqueous media, Iran. J. Chem. Chem. Eng., 36 (2017) 1–9.
[34] N. Kannan, M.M. Sundaram, Kinetics and mechanism of removal of Methylene blue by adsorption on various carbons — a comparative study, Dyes Pigm., 51 (2001) 25–40.
[35] A. Elsagh, O. Moradi, A. Fakhri, F. Najafi, R. Alizadeh, V. Haddadi, Evaluation of the potential cationic dye removal using adsorption by graphene and carbon nanotubes as adsorbents surfaces, Arabian J. Chem., 10 (2017) S2862–S2869.
[36] A.F. Alkaim, Z. Sadik, D.K. Mahdi, S.M. Alshrefi, A.M. Al-Sammarraie, F.M. Alamgir, P.M. Singh, A.M. Aljeboree, Preparation, structure and adsorption properties of synthesized multiwall carbon nanotubes for highly effective removal of Maxilon Blue dye, Korean J. Chem. Eng., 32 (2015) 2456–2462.
[37] Y. Nuhoglu, E. Malkoc, Thermodynamic and kinetic studies for environmentally friendly Ni(II) biosorption using waste pomace of olive oil factory, Bioresour. Technol., 100 (2009) 2375–2380.
[38] C.H. Weng, Y.T. Lin, T.W. Tzeng, Removal of Methylene blue fro aqueous solution by adsorption onto pine apple leaf powder, J. Hazard. Mater., 170 (2009) 417–424.
[39] C.R. Minitha, M. Lalitha, Y.L. Jeyachandran, L. Senthilkumar, R.T.R. Kumar, Adsorption behaviour of reduced graphene oxide towards cationic and anionic dyes: co-action of electrostatic and π–π interactions, Mater. Chem. Phys., 194 (2017) 243–252.